



Science Arts & Métiers (SAM)

is an open access repository that collects the work of Arts et Métiers Institute of Technology researchers and makes it freely available over the web where possible.

This is an author-deposited version published in: <https://sam.ensam.eu>
Handle ID: <http://hdl.handle.net/10985/17941>

To cite this version :

Eskandar MOUNIF, Véronique BELLENGER, Philippe MAZABRAUD, Fabien NONY, Abbas TCHARKHTCHI - Chemorheological study of DGEBA/IPD system for Reactive Rotational Molding (RRM) - Journal of Applied Polymer Science - Vol. 116, n°2, p.969-976 - 2010

Any correspondence concerning this service should be sent to the repository

Administrator : scienceouverte@ensam.eu



Chemorheological Study of DGEBA/IPD System for Reactive Rotational Molding (RRM)

E. Mounif,¹ V. Bellenger,¹ P. Mazabraud,² F. Nony,² A. Tcharkhtchi¹

¹ENSAM, 151 Bd de l'Hôpital, 75013 Paris, France

²CEA Ripault, BP 16, 37260 Monts, France

ABSTRACT: The identification of kinetic parameters controlling the crosslinking of Diglycidyl ether of bisphenol/isophorone diamine reactive system was achieved via optimization program (Inverse method) based on Fourier transform near infrared spectroscopy results. The reactivity ratio (k_2/k_1) was determined using a new method based on the variation of amine conversion ratio versus epoxy conversion ratio. Gelation and

vitrification of the reactive system were also analyzed. Time, temperature, transformation diagram was established to assess the rotational molding of this reactive system. © 2009 Wiley Periodicals, Inc. *J Appl Polym Sci* 116: 969–976, 2010

Key words: gelation; rotational molding; kinetic crosslinking; TTT diagram; epoxy/amine

INTRODUCTION

The diglycidyl ether of bisphenol A (DGEBA)/isophorone diamine (IPD) epoxy amine system was the subject of many research papers.^{1–3} The optimization of reactive rotational molding^{4–6} of such system requires the analysis of the structure evolution. During gelation, a three-dimensional infinite network is formed and accompanied by an increase in viscosity ($\eta \rightarrow \infty$) due to the increase of molar weights. The gel point marks the limit of the processing. In the case of the reactive rotational molding, the shape of the part should be formed before gelation. An optimal interval of viscosity should be reached before the gel point. Although the gelation is controlled by the reaction between the largest reduced mobility clusters, the pre gel is characterized by the formation of low molecular weight oligomers. The required crosslinking temperature ($T_C < 100^\circ\text{C}$) for the DGEBA/IPD epoxy/amine reactive system is low when compared with other aromatic amine hardener systems, which limits the thermal effect on viscosity and makes it a good choice for rotational molding.

To determine the processing possibility of such systems by rotational molding, a rheological and thermal analysis was achieved in parallel with an infrared spectroscopy to investigate the structural

modification of the reactive system during crosslinking. The time-temperature-transformation (TTT)⁷ diagram helps us to explore the different phases of the reactive system, especially the succession of gelation and vitrification.

Crosslinking kinetic

Because of the different structural environments of aliphatic and cyclo aliphatic primary amine groups of the hardener, one has to take into account the difference of reactivity between these groups and between the resulted secondary amines. The difference of reactivity of the cis and trans conformation was studied by Lopez-Quintela et al.⁸ They showed that these two conformations do not have the same reactivity. To be able to well describe the kinetics of the crosslinking reaction, we have to consider several kinetic parameters, which make the problem very hard to solve.

Figure 1 shows the steps of the mechanism of crosslinking with the corresponding kinetic parameters $k_i, k'_i, k_{ic}, k'_{ic}$, $i = 1, 2$.

The following approximations are considered to model the kinetic of DGEBA/IPD crosslinking in the pre gel phase:

1. Aliphatic and cycloaliphatic amine groups have same reactivity, which means: $k_i = k'_i$, $k_{ic} = k'_{ic}$, $i = 1, 2$.
2. Primary amine group has a higher reactivity than secondary one. The difference of reactivity can be demonstrated by DSC dynamic scans.⁹

Correspondence to: A. Tcharkhtchi (abbas.tcharkhtchi@paris.ensam.fr).

(a)

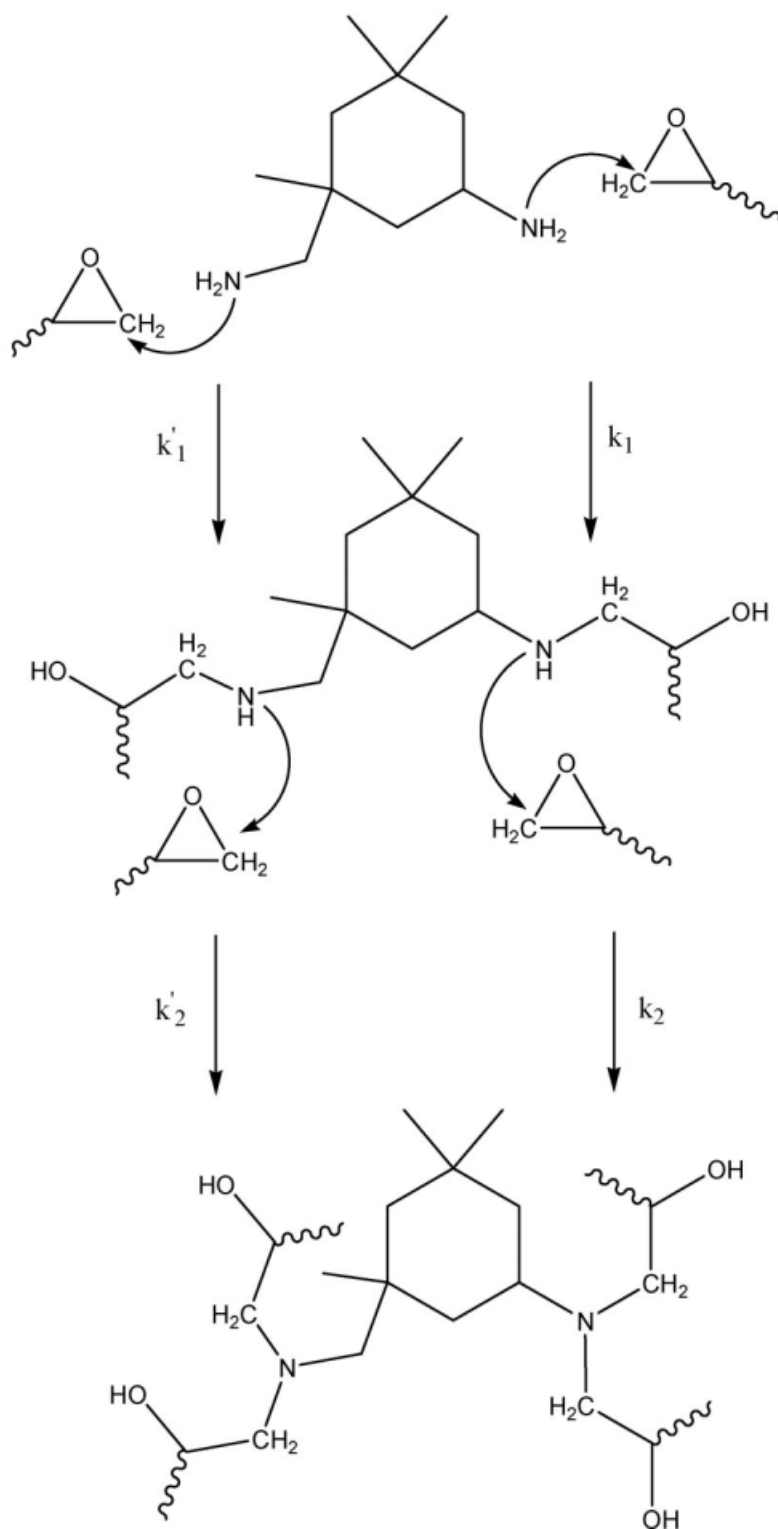


Figure 1 (a) Noncatalytic and (b) catalytic mechanism of epoxy/amine crosslinking.

- We assume only one single reactivity ratio for both catalytic and noncatalytic mechanism (i.e., $r = \frac{k_2}{k_1} = \frac{k_{2c}}{k_{1c}}$).
3. The activation of epoxy group (E) by hydroxyl group (OH) (auto catalyzation) is a rapid preequilibrium.
 4. No side reactions (i.e., etherification) or cyclization occur during the crosslinking.
 5. cis and trans conformation of the IPD hardener have same reactivity.
 6. Both epoxy groups of the DGEBA have same reactivity.

(b)

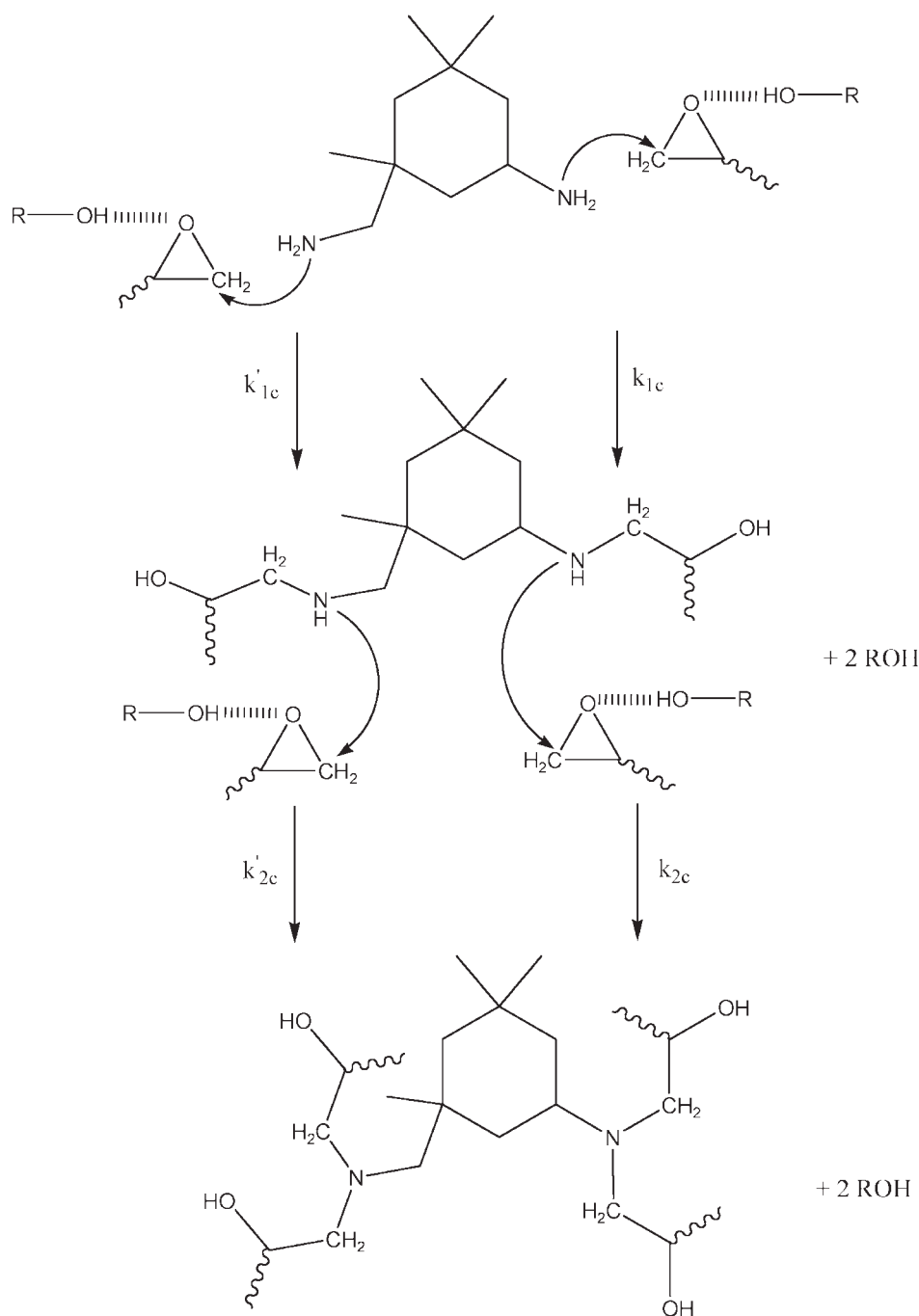


Figure 1 (Continued)

7. Diffusion of reactants has no effect on the reaction kinetics.¹

In this case, differential equations controlling the kinetic of the crosslinking can be simplified to:

$$\begin{aligned} \frac{d[E]}{dt} &= -k_1[A_1][E] - k_2[E][A_2] - k_{1c}[A_1][E][OH] \\ &\quad - k_{2c}[E][A_2][OH] \\ \frac{d[A_1]}{dt} &= -k_1[A_1][E] - k_{1c}[A_1][E][OH] \end{aligned} \quad (1)$$

Where $[E]$, $[A_1]$, $[A_2]$, $[OH]$ are, respectively, concentrations of epoxy, primary amine, secondary amine, and hydroxyl group (Fig. 2). Secondary amine and hydroxyl groups can be obtained from the following conservation equations:

$$\begin{aligned} [A_2] &= 2([A_1]_0 - [A_1]) - ([E]_0 - [E]) \\ [OH] &= [OH]_0 + [E]_0 - [E] \end{aligned} \quad (2)$$

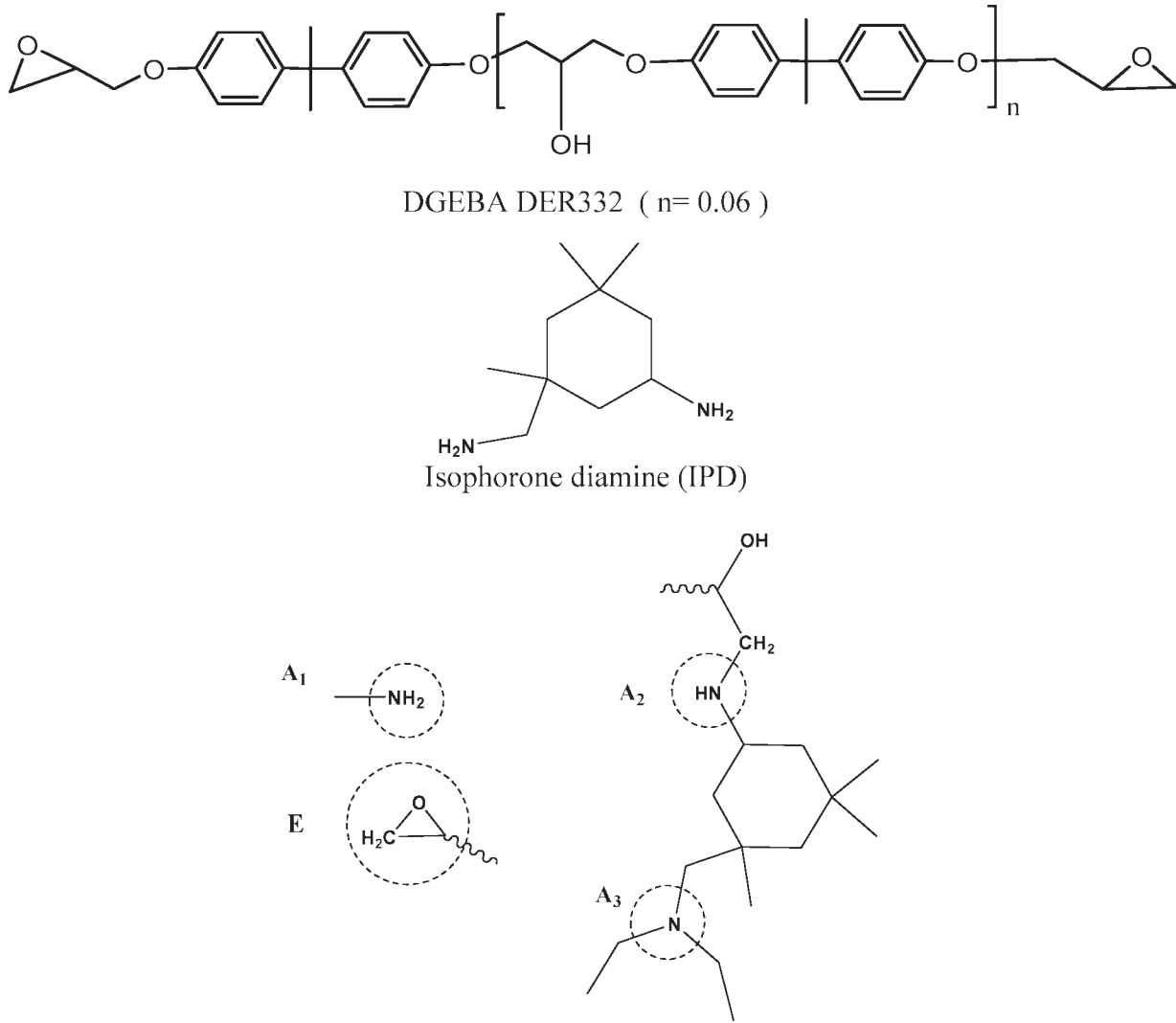


Figure 2 Chemical structure of epoxy DGEBA and the diamine hardener IPD and chemical group symbols.

Estimation of substitution effect

If we consider the autocatalytic mechanism (1) of crosslinking, the variation of amine group conversion ratio relative to epoxy one ($\frac{dx_{A_1}}{dx_E}$) can be expressed as:

$$\frac{dx_{A_1}}{dx_E} = \frac{2(x_{A_1} - 1)}{(x_{A_1} - 1) + 2r(x_E - x_{A_1})} \quad (3)$$

Epoxy and primary amine conversion ratios are defined as $x_E = \frac{[E]_0 - [E]}{[E]_0}$, $x_{A_1} = \frac{[A_1]_0 - [A_1]}{[A_1]_0}$.

The advantage of the last eq. (3) is its time independence. The ratio ($\frac{dx_{A_1}}{dx_E}$) can be estimated as the slope of the $x_{A_1} = f(x_E)$ curve and compared to the second hand side of the eq. (3) to estimate the reactivity ratio (r) at that point.

Viscosity variation

Several approaches were used in literature¹⁰ to model the variation of rheological properties near the gel point. The Castro-Macosko model¹¹ is the most popular one. It describes the variation of viscosity near the gel point as a function of the conversion ratio (4). The use of the reduced dynamic shear viscosity ($\frac{\eta}{\eta_0}$) can eliminate temperature or catalyst concentration dependence.¹² In the case of the DGEBA/IPD reactive system, the constants A and B were found to be dependant on crosslinking temperature.¹

$$\left(\frac{\eta}{\eta_0}\right) = \left(\frac{x_{\text{gel}}}{x_{\text{gel}} - x}\right)^{A+Bx} \quad (4)$$

The Castro-Macosko model is valid near the gel point where the behavior of the reactive system is

controlled by the fractal nature of diffusing clusters,¹³ but it cannot be used to describe the initial steps of crosslinking. In the case of branched macromolecules, the scaling law (5) links the viscosity to molar weight is suggested:

$$\eta = K(g\overline{M}_w)^a \quad (5)$$

With g , the ratio of the radius of gyration of a branched macromolecule to the one of a linear macromolecule having the same molar weight \overline{M}_w .¹⁴ During the initial steps of the crosslinking, entanglements do not exist and the scaling law (5) fails to model the viscosity-weights relationship. In fact, the polydispersity and branched structure make it difficult to find an efficient scaling law.

Dual Arrhenius model¹⁵ is a practical equation to describe the time and temperature dependence of the viscosity. According to this model the viscosity can be expressed as:

$$\eta(T, t) = \eta_0 e^{kt} \quad (6)$$

With η_0 is the isothermal viscosity, k is a global kinetic parameter. If the parameters k and η_0 can be written as $k = k_0 e^{\frac{\Delta E_k}{RT}}$, $\eta = \eta_\infty e^{\frac{\Delta E_\infty}{RT}}$ with ΔE_k , ΔE_∞ are, respectively, chemical and flow activation energy, eq. (6) can be written as:

$$\ln \eta(T, t) = \ln \eta_\infty + \frac{\Delta E_\eta}{RT} + k_0 e^{\frac{\Delta E_k}{RT}} t \quad (7)$$

EXPERIMENTAL

Materials

DGEBA with an epoxy equivalent weight of 178 g mol⁻¹ from Fluka is used. IPD with an N—H equivalent mass of 42.6 g mol⁻¹ is added as a hardener. Figure 2 represents the chemical structures of both components. To prepare the thermoset system, hardener is added to DGEBA in stoichiometric ratio. To obtain a homogenous mixture, the components are mixed quickly and degassed under vacuum for few minutes at room temperature.

Methods

Rheological analysis

The viscosity variation and gel point determination were achieved using ARES Rheometer from TA instrument equipped with parallel plates with a 0.5–1 mm spacing and a 50 mm diameter. The reactive mixture is added quickly on the preheated plate and a time sweep is started when the temperature equilibrium was reached again. A time ramp at a multi-frequency mode ($f = 0.25, 1, 2$, and 5 Hz) is used to determine the gel time considering Winter crite-

ron.^{16,17} According to this criterion, the gel point is reached when the loss factor is independent of frequency.

Thermal analysis

The cure of investigated systems is studied by means of a differential scanning calorimeter DSC-Q10 from TA instruments, using aluminum hermetic crucibles. The DSC is calibrated in enthalpy and temperature scales by using a high purity indium sample. Interrupted isothermal crosslinking was achieved *in situ* in the DSC cell in sealed aluminum crucibles. Crosslinking is quenched by a rapid cooling when the desired crosslinking time is reached. To measure the residual enthalpy and glass transition temperature T_g , a dynamic scan (5°C min⁻¹) was achieved. The total heat of reaction, $\Delta H_0 = 424$ J g⁻¹, is estimated by integrating the exothermal peaks of the uncured sample.

Near infra red (NIR) spectroscopy

Fourier transform near infrared spectroscopy (FTNIR) is performed using Bruker IFS28 spectrophotometer, equipped with a Globar source, KBr beam splitter, and DTGS detector. All spectra were collected in the near infrared domain (7500–4000 cm⁻¹) at a 4 cm⁻¹ resolution and 32 scans per sample. For thermal control, a temperature controller is used (Specac). The reactive mixture is injected with a syringe in the cell (Quartz with 2 mm path-length) when the controller showed the programmed temperature. In our case, the same cell is used for all experiments; therefore, we applied the simple equation: $x_{\text{NIR}} = 1 - \frac{A_t}{A_0}$, to quantify the chemical group conversion ratio; A_t/A_0 is the ratio of the actual area/height of peak with respect to the initial one. In our case, height of peaks (epoxy at 4529 cm⁻¹, primary amine at 4923 cm⁻¹)^{18,19} is used to quantify its conversion ratios.

RESULTS AND DISCUSSION

Kinetics parameters

Substitution effect (r)

The dynamic DSC scans (5°C min⁻¹) of the partly crosslinked ($T_{\text{cure}} = 50^\circ\text{C}$) samples shows (Fig. 3) two shouldered peak ($T_1 = 98^\circ\text{C}$ and $T_2 = 125^\circ\text{C}$) attributed, respectively, to the primary and secondary amines. It was experimentally demonstrated²⁰ that the second peak disappears if an excess of amine hardener (IPD) is used, which proves that IPD has an important negative substitution effect ($r = \frac{k_2}{k_1}$).

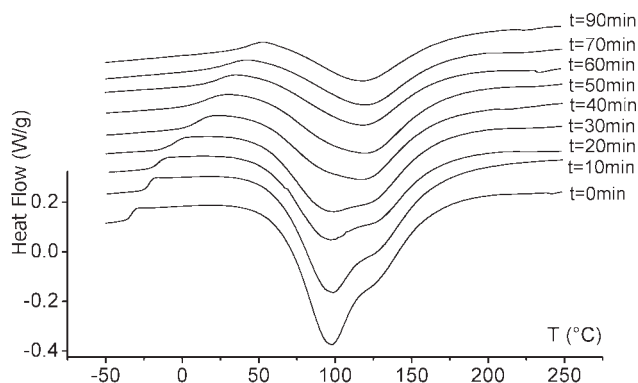


Figure 3 DSC dynamic scans (5°C/min) of partly cured samples (50°C) for 0, 10, 20, 30, 40, 60, 70, and 90 min) of the DEGBA/IPD system. Thermograms are shifted to make the figure reading easier.

The near infrared spectroscopy is an efficient technique to determine the substitution effect. The conversion ratio of primary amine and epoxy groups can be measured simultaneously (Fig. 4).

Using the maximum concentration of secondary amine groups Paz et al.³ have developed an experimental method to measure the substitution effect (r). In fact, the determination of secondary amine conversion ratio could not be achieved directly from near infrared results because its peak (6400–6800 cm^{-1}) is overlapped with the primary amine one. We need to use a proper deconvolution method²¹ of the combined absorption peak. Using conservation equations to deduce the concentration of secondary amines is limited by the determination of the primary amine conversion ratio which becomes hard to measure at the final steps ($x_{A_1} \rightarrow 1$) because of the baseline shift (Fig. 4). In fact, the secondary amine concentration is maximal when the primary amine conversion ratio is about 90%.

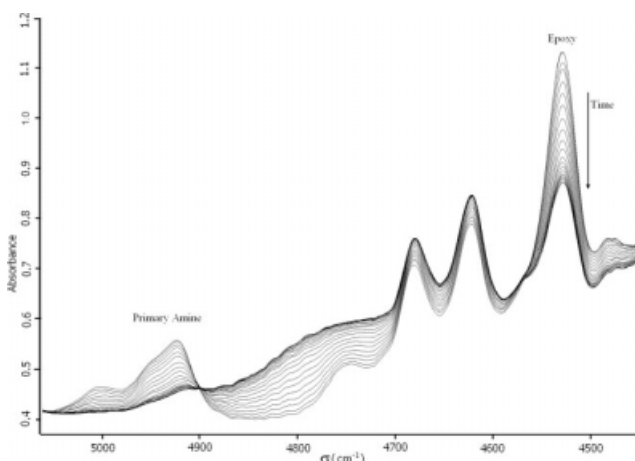


Figure 4 Collected near infrared spectra during DGEBA/IPD cross linking at 22°C.

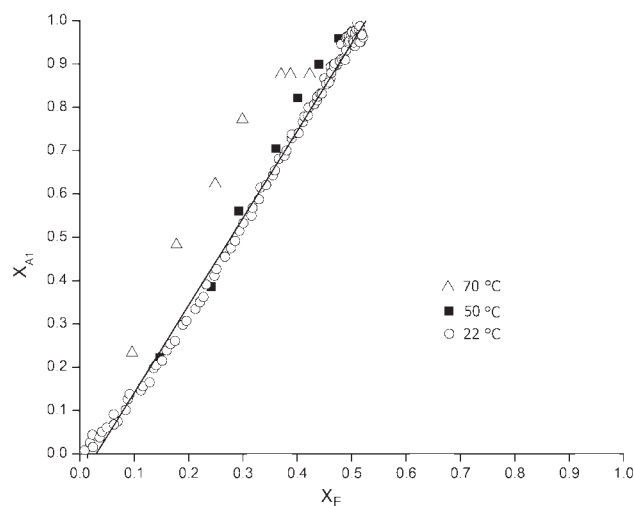


Figure 5 Primary amine conversion ratio versus epoxy conversion ratio during isothermal crosslinking (22, 50, and 70°C), for DGEBA/IPD system as obtained by NIR spectroscopy.

So, we established a new method for measuring the substitution effect by using the variation of the primary amine conversion versus epoxy conversion ratios ($x_{A_1} = f(x_E)$) without the need to consider the secondary amine groups conversion ratio. Figure 5 represents the variation of x_{A_1} versus x_E for the isothermal crosslinking experiments. The curves are almost superimposed for the used temperatures, which means that the same mechanism is followed regardless the crosslinking temperature. The same conclusion was achieved by Varley et al.²² who extended their study to the reaction between the secondary amine and epoxy groups.

A mean value of r can be calculated also by seeking the solution of the differential Eq. (1) which fits the best experimental result.

The obtained values of reactivity ratio (Table I) are very low compared with those of other amine hardeners.²¹ As the DSC and NIR results confirm, the primary amine reaction is dominant when compared with the secondary amine/epoxy reaction in the pre-gel phase. This can be explained by the bulky structure of the amine hardener. So, we considered only the primary amine as the main one to model the kinetics of DGEBA/IPD crosslinking reaction, which reduces the number of kinetic parameters to two (k_1 , k_{1c}).

TABLE I
Reactivity Ratio for Primary and Secondary Amine of IPD at Different Temperatures

T_C (°C)	r
22	0.03
50	0.01
70	0.00

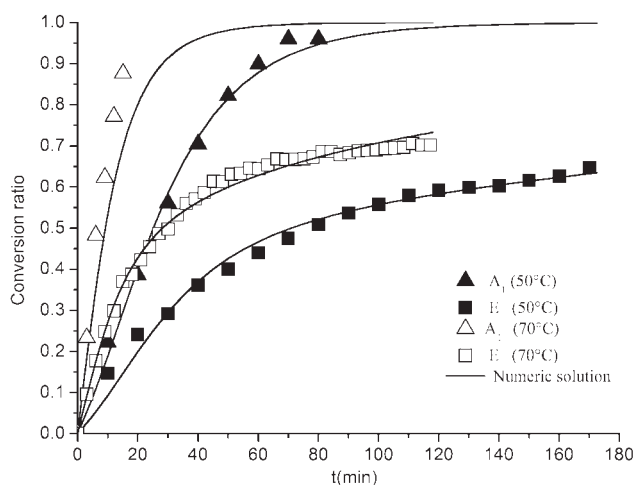


Figure 6 Conversion ratios of amine and epoxy groups during isothermal crosslinking at 50 and 70°C determined by near infra red spectroscopy. The numeric solution was limited to the chemical kinetic control domain to avoid diffusion effect on the obtained kinetic parameters.

Kinetic parameters of catalytic and noncatalytic mechanism

We used an inverse method based on Runge-Kutta method to find the numeric solution of the differential equation and the direct search method²³ for optimization. The kinetic parameters (k_1 and k_{1c}) are obtained as the best fit of near infrared spectroscopy results (Fig. 6).

By using only two kinetic parameters (k_1 and k_{1c}), a good fit is obtained. The auto-catalytic mechanism is dominant ($k_{1c} > k_1$) for low crosslinking temperatures (22, 50°C) (Table II). As the research of the kinetic parameters is limited to pregel phase, they will not be meaningful after the gel point.

Vitrification

Measuring the glass transition temperature T_g during the isothermal crosslinking allows us to estimate the time to vitrification ($t = t_{vit}$ when $T_g = T_c$) with T_c the crosslinking temperature.

The dependence of glass transition temperature on viscosity is considered using a classical Di Benedetto equation $T_g = T_{g0} + \frac{\lambda(T_{g\infty} - T_{g0})x}{1 - (1 - \lambda)x}$ with $T_{g0} = -33^\circ\text{C}$, $T_{g\infty} = 153^\circ\text{C}$, and $\lambda = 0.36$.¹

TABLE II
Kinetic Parameters of Isothermal Crosslinking of DGEBA/IPD System Determined by Optimisation of NIR Results

T_c (°C)	k_1 (kg mol ⁻¹ min ⁻¹)	k_{1c} (kg ² mol ⁻² min ⁻¹)
22	—	0.9×10^{-3}
50	2.3×10^{-3}	7×10^{-3}
70	11.8×10^{-3}	9.8×10^{-3}

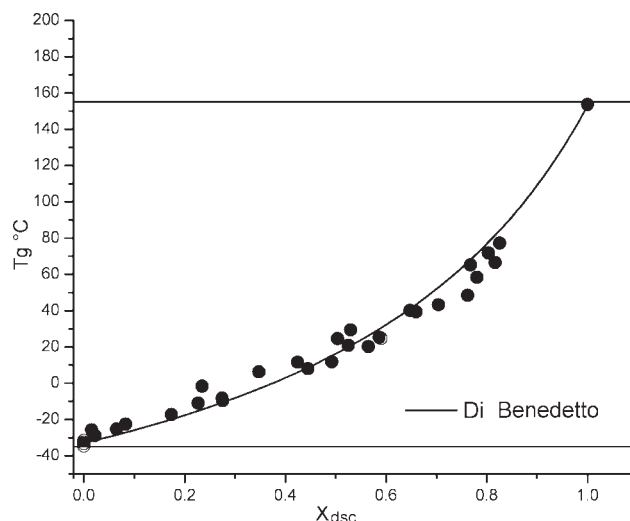


Figure 7 Glass transition temperature versus conversion ratio for DGEBA/IPD.

The result of this modeling (Fig. 7) is in good agreement with reported results in literature.¹ This direct relationship between the glass transition temperature and the conversion ratio is a good tool to estimate a conversion ratio via measuring the glass transition temperature regardless the thermal program done on the crosslinked sample.

Rheological analysis and TTT diagram

Viscosity variation

Figure 8 shows the variation of dynamic shear viscosity during an isothermal crosslinking of the DGEBA/IPD system at 50, 60, and 70°C (only results for 1 Hz are showed). The variation of dynamic shear viscosity can be divided in two main intervals: initial, and near gel point domains. In fact, the viscosity is proportional to the molar weights of oligomers and for linear polycondensation, high

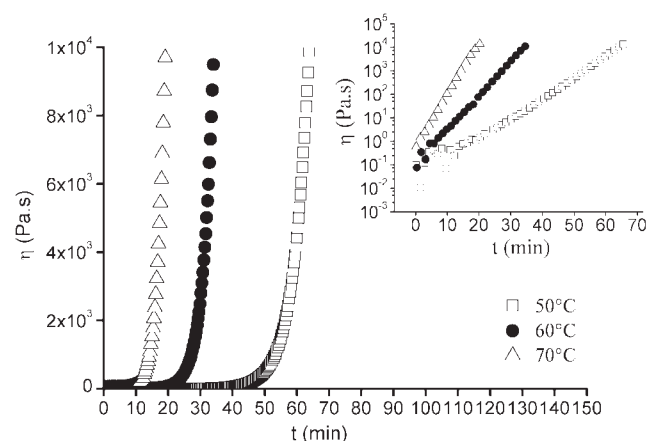


Figure 8 Viscosity evolution during isothermal (50, 60, and 70°C) crosslinking of DGEBA/IPD.

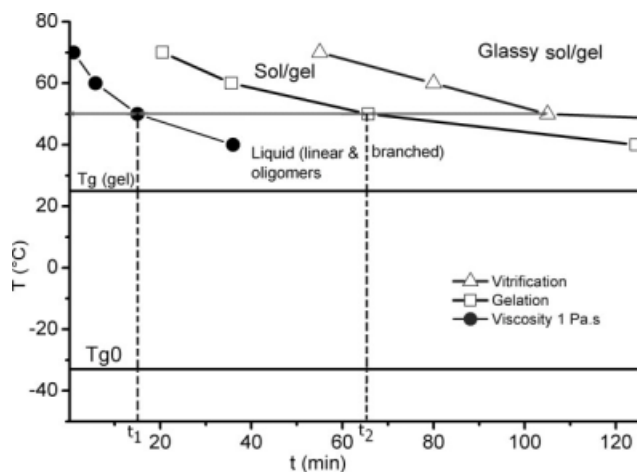


Figure 9 Isothermal TTT diagram for DGEBA/IPD system with iso-viscosity curves measured at 1 Hz.

molar weights are formed only for high conversion ratio (Average polymerization degree is given by $DP_n = \frac{1}{1-x}$, x : conversion ratio) which means that for initial steps, the viscosity will be relatively low especially with the formation of branches [viscosity is higher for linear polymer when compared with the branched equivalent one (same \overline{M}_w)].

The dual Arrhenius model was applied to the DGEBA/IPD system. The identified chemical activation energy ($\Delta E_k = 16 \text{ kJ} \cdot \text{mol}^{-1}$) is lower than the flow activation energy ($92 \text{ kJ} \cdot \text{mol}^{-1}$) which is in agreement with reported value in literature.^{15,24} The constant k quantifies the global crosslinking effect but unfortunately no explicit relationship has been proved between k and the kinetic parameters (k_1 , k_{1c}) of the auto catalytic mechanism.

TTT diagram

The isothermal TTT diagram of the DGEBA/IPD epoxy/amine system was established (Fig. 9) by regrouping rheological and thermal analysis results. The fitting of gel time by the Arrhenius equation gives us the corresponding activation energy of $E_a = 54 \text{ kJ} \cdot \text{mol}^{-1}$, which is in agreement with the most published²⁵ value.

To determine the processability window in term of viscosity [η_{\min} , η_{\max}] for rotational molding, we added the isoshear dynamic viscosity curves to the TTT diagram. These curves help us to estimate the time to reach certain viscosity value and to define the domain of rotational molding for the DGEBA/IPD system.

We considered the viscosity of 1 Pa.s as reference minimal viscosity, to compare the processability window of reactive systems. The DGEBA/IPD and systems show a manageable pot life with relatively higher viscosity than the (DGEBA/DETDA)²³ system. The corresponding time cycle is presented on the TTT diagram. The rotation is efficient only for (t_1

$< t < t_2$), with t_1 time to reach the viscosity of 1 Pa.s, t_2 is the gel time.

CONCLUSION

The isothermal crosslinking of the DGEBA/IPD epoxy/amine reactive system was analyzed by near infrared spectroscopy. A new method was established to estimate the substitution effect (r) from the variation of x_{A_1} versus x_E determined by near infrared spectroscopy. The kinetic parameters (k_1 , k_{1c}) of the catalytic and noncatalytic system were identified during the pregel phase without taking into account the vitrification effect. The gelation and vitrification of reactive system were studied and results were regrouped on the TTT diagram. The isoviscosity curve helped us to limit the rotational molding domain on the TTT diagram. Dual Arrhenius model was used to model viscosity variation versus time and temperature.

References

- Pichaud, S.; Duteurtre, X.; Fit, A.; Stephan, F.; Maazouz, A.; Pascault, J. P. *Polym Int* 1999, 48, 1205.
- Sabra, A. Ph.D. Thesis, INSA Lyon (1995).
- Paz-Abuin, S.; Lopez-Quintela, A.; Varela, M.; Pazos-Pellin, M.; Prendes, P. *Polymer* 1997, 38, 3117.
- Crawford, R. J.; Throne, J. L. *Rotational Molding Technology*; Plastics Design Library: New York, 2002.
- Nugent, P. *Handbook of Plastic Processes*; Wiley: New Jersey, 2006; p387.
- Corrigan, N.; Harkin-Jones, E.; Brown, E.; Coates, P. D.; Crawford, R. J. *Plast Rubber Compos* 2004, 33, 37.
- Enns, J. B.; Gillham, J. K. *J Appl Polym Sci* 1983, 28, 2567.
- Lopez-Quintela, A.; Prendes, P.; Pazos-Pellin, M.; Paz, M.; Paz-Abuin, S. *Macromolecules* 1998, 31, 4770.
- Sabra, A.; Lam, T. M.; Pascault, J. P.; Grenier-Loustalot, M. F.; Grenier, P. *Polymer* 1987, 28, 1030.
- Halley, P. J.; Mackay, M. E. *Polym Eng Sci (USA)* 1996, 36, 593.
- Castro, J. M.; Macosko, C. W. *SPE Tech Pap* 1980, 26, 434.
- Bidstrup, S. A.; Macosko, C. W. *J Polym Sci Part B: Polym Phys* 1990, 28, 691.
- Somvarkar, J.; Dušek, K.; Smrckova, M. 1998, 8, 201.
- Miller, D. R.; Macosko, C. W. *Macromolecules* 1980, 13, 1063.
- Tungare, A. V.; Martin, G. C.; Gotro, J. T. *Polym Eng Sci* 1988, 28, 1071.
- Chambon, F.; Winter, H. H. *J Rheol* 1987, 31, 683.
- Matejka, L. *Polym Bull* 1991, 26, 10.
- Poisson, N.; Lachenal, G.; Sautereau, H. *Vib Spectrosc* 1996, 12, 237.
- Mezzenga, R.; Boogh, L.; Manson, J. A. E.; Pettersson, B. *Macromolecules* 2000, 33, 4373.
- Sabra, A.; Pascault, J. P.; Seytre, G. *J Appl Polym Sci* 1986, 32, 5147.
- Liu, H.; Uhlherr, A.; Varley, R. J.; Bannister, M. K. *J Polym Sci Part A: Polym Chem* 2004, 42, 3143.
- Varley, R. J.; Heath, G. R.; Hawthorne, D. G.; Hodgkin, J. H.; Simon, G. P. *Polymer* 1995, 36, 1347.
- Mounif, E.; Bellenger, V.; Tcharkhtchi, A. *J Appl Polym Sci* 2008, 108, 2908.
- Martin, G. C.; Tungare, A. V.; Gotro, J. T. *Polym Eng Sci* 1989, 29, 1279.
- Ishii, Y.; Ryan, A. J. *Macromolecules* 2000, 33, 158.